Climate Warming related strengthening of the tropical hydrological cycle

Matthias Zahn * and Richard Allan

University of Reading, Reading, United Kingdom

* *Corresponding author address:* Matthias Zahn, Environmental Systems Science Centre, University of Reading, Harry Pitt Building, 3 Earley Gate, Reading RG6 6AL, U.K.

E-mail: m.zahn@reading.ac.uk

ABSTRACT

We estimate climate warming related 21st century changes of moisture transports from the descending into the ascending regions in the tropics. Unlike previous studies which employ time and space averaging, we here use homogeneous high horizontal and vertical resolution data from an IPCC-AR4 climate model. This allows for estimating changes in much greater detail, e.g. the estimation of the distribution of ascending and descending regions, changes in the vertical profile and separating changes of the inward and outward transports. We found low level inward and mid-level outward moisture transports of the convective regions in the tropics increase in a simulated anthropogenically warmed climate as compared to a simulated 20th century atmosphere, indicating an intensification of the hydrological cycle. Since an increase of absolute inward transport exceeds the absolute increase of outward transport the resulting budget is positive, meaning that more water is projected to converge in the moist tropics. The intensification is found mainly to be due to the higher amount of water in the atmosphere, while the contribution of weakening wind counteracts this response marginally. In addition we here investigate the changing statistical properties of the vertical profile of the moisture transport and demonstrate the importance of the substantial outflow of moisture from the moist tropics at mid-levels.

1. Introduction

Future changes in the tropical hydrological cycle (Trenberth et al. 2007; Bengtsson 2010) may alter the distribution of available fresh water regionally through altered moisture transport properties and precipitation minus evaporation patterns (Allen and Ingram 2002; Trenberth et al. 2003). The atmospheric part of the hydrological cycle is to a large extent determined by the large scale circulation patterns. In the tropics these consist of convective regions of upward, ascending air movement (ASC) and of regions of downward, descending air motion (DESC), with low-level flow into ASC and mid-level outflow into DESC commonly referred to as the Hadley Cell circulation. Atmospheric moisture precipitates in ASC as air rises upward.

A key response in a warmed atmosphere is an increase of low-level atmospheric water vapor of 7% per degree of warming derived from theoretical considerations (Clausius-Clapeyron relation, e.g. Wentz and Schabel (2000); Trenberth et al. (2003); Held and Soden (2006); O'Gorman and Muller (2010)), with a strengthening impact on moisture transports and on precipitation. Precipitation generally has been found to increase with warming in the ascending tropical regions (Chou et al. 2007; John et al. 2009), and is expected to increase especially in extreme events, which were found to increase stronger than average (Kharin et al. 2007; Lenderink and van Meijgaard 2008; Allan and Soden 2008). However, models may have deficiencies representing the increase adequately (O'Gorman and Schneider 2009) and in agreement with observations (Allan and Soden 2007; Allan et al. 2010). Over the course of the annual cycle Chou et al. (2007) found precipitation increase in warm and wet seasons, but found the cooler dry seasons to become slightly drier as the atmosphere warms.

Generally climate warming related changes changes of transported moisture are mainly explained by thermodynamic arguments, higher specific humidity in a warmer atmosphere, and the dynamic part, wind circulation is generally considered less important (Emori and

Brown 2005; Seager et al. 2010). Using different measures a couple of studies have suggested the tropical circulation part to weaken (Vecchi et al. 2006; Power and Smith 2007; Gastineau and Soden 2009; Chou and Chen 2010). However there have also been a couple of studies reporting the opposite, a strengthening of the circulation, at least for the past (Bigg 2006; Sohn and Park 2010; Zahn and Allan 2011).

Most of these studies are estimates based on low resolution re-analysis data, low resolution climate model data or observation based point measurements. Applying space or time averaged values was found to be insufficient in one of our recent studies (Zahn and Allan 2011) and may lead to wrong numbers for the moisture transport. We thus here re-investigate climate warming related changes of water vapor transports into the ascending regions of the tropics by applying high-resolution data from an IPCC-AR4 model. Unlike the methods in the above mentioned studies, we base our investigations not only on low resolution time and/or spatial mean values but also on the six-hourly output of the high horizontal and vertical resolution simulation.

2. Data and method

We used six-hourly T213 (0.5°) horizontal resolution ECHAM5 model (Roeckner et al. 2003) data at 31 vertical levels representative for two time slices of 31 years, 1959-1989 (C20) and 2069-2099 (C21). The simulations are of the time slice type forced with boundary data (Sea Surface Temperature and Sea Ice) from a coupled climate simulation with the same model at T63 resolution. The C20 uses observed Greenhouse Gas and aerosol forcing, the C21 forcing was delivered by the A1B scenario (Nakicenovic and Swart 2000) of the Fourth Assessment Report (AR4) of the Intergovernmental Panel of Climate Change (IPCC). We used vertical (ω) and horizontal ($\mathbf{U}$,$\mathbf{V}$) wind vectors, specific humidity (q) and surface air pressure for all 31 model levels (from the surface up to the top of the atmosphere) in a two-staged approach for calculating the moisture transports:

- in model results of both, C20 and C21, we identified regions of ascending and of descending ω and defined the boundary separating both
- in model results of both, C20 and C21, we identified $\mathbf{U}$, $\mathbf{V}$, humidity and pressure at each level along the boundary and calculated the moisture transport

This method has been adapted from an earlier study applying re-analysis data (Zahn and Allan 2011) and is described in more detail in the following subsections.

Definition of Ascending and Descending regions and of the boundary in between

To define ascending and descending regions at each grid cell in the tropical region between $-30°$ and $30°$ latitude the sum of the vertical wind motion ω of the lower and middle part of the atmosphere, the lowest 21 model levels corresponding to a height of up to approximately $450hPa$ was estimated. Before summing up, the vertical motion representative for each level is weighted by the thickness of each level. Grid boxes with an upwards directed overall ω are assigned to the ascending region (ASC), else, if $\omega = 0$ or directed downwards they are assigned to the descending regions (DESC). The boundary over which moisture transports are estimated is defined as the line separating ASC and DESC. If ASC or DESC is cut by the $-30°$ or $30°$ latitude line, an artificial boundary is drawn along this latitude to avoid 'open' regions.

ASC and DESC are estimated based on monthly mean ω, resulting in 372 (one per month over 31 years) different ASC/DESC masks, as well as on instantaneous ω representative for the 180 seconds of the calculation time step in the ECHAM5 model, resulting in ≈ 45280 (one per time step over 31 years) different ASC/DESC masks. Example fields of both are shown in Fig. 1. Please note that while the mean ASC/DESC masks reflect the general pattern of the

Intertropical Convergence Zone (ITCZ) with ASC stretching along the equator, the instantaneous field exhibits a much more complex pattern of convective cells and down-draft regions.

Calculation of moisture transports

At each time step t the moisture transport is calculated across all the n_b boundary segments b between ASC and DESC (green lines in Fig. 1) at each of the n_l vertical model levels l by multiplying the perpendicular wind vector (WP) with the precipitable water content (PWC), respectively. The resulting total moisture transport (MT) per time step then reads:

$$MT_t = \sum_{b}^{n_b} \sum_{l}^{n_l} WP_{bl} \cdot PWC_{bl} \tag{1}$$

Since applying mean wind speeds and mean PWC has proven to be insufficient previously (Zahn and Allan 2011), the calculations were only conducted using instantaneous variables. This leads to four experiments, moisture transports into monthly mean ascending regions (denoted ASC_m) and into instantaneous ascending regions (denoted ASC_i) for the 20th and 21st century, respectively. Please note that as a consequence of the four times daily instantaneous values, we do not have a continuous integration of instantaneous moisture flux but rather a set of four observations per day. We should also note that in the C21 output the fields at three time steps, at 18 Jan 2077 12:00 , at 18 Jan 2077 18:00 and at 31 Aug 2079 18:00 were corrupt. They were replaced by the data at 18 Jan 2077 06:00, at 19 Jan 2077 00:00 and at 31 Aug 2079 12:00, respectively.

3. Results

Changes of the vertical profile of moisture transport

The average vertical profile of transports along the boundary of ascending (ASC) and descending regions (DESC) in all experiments and in high resolution re-analysis based comparison data from ERA-interim (Dee et al. 2011; Zahn and Allan 2011) is dominated by a maximum of inward transports at the lower levels, but a considerable outward one (negative values) is visible as well above a certain reversal level (RL, Fig. 2). RL is defined as the level at which moisture transport is $MT = 0$, and $MT < 0$ above and $MT > 0$ below. Despite a bias in the absolute numbers, the modeled profiles agree well with the re-analysis based ones. All of them correspond well with expected moisture transports, which follow the Hadley circulation pattern and are directed towards ASC at the lower levels, and outwards at the mid-levels. In the ASC_m as well as in the ASC_i experiments the inward moisture transports at the lower levels as well as the mid-level outflow are more intense in C21 as in C20.

Contrary to the idealized view on the Hadley Circulation the air flow is not directed towards the convective regions at all boundary segments at all times in the instantaneous wind fields, neither in ASC_i nor ASC_m. Rather, if isolated, inward and outward transport have a similar vertical shape (Fig. 3), which seems to be determined by the vertical distribution of moisture in the atmosphere. A weaker outward than inward transport at lower levels, and, vice versa, a stronger outward than inward transport at mid-levels, results in the expected shape of the mean vertical profile.

Both ways of defining the convective regions (ASC_m and ASC_i) result in an increase of accumulated overall inward transport as well as in an increase of the accumulated overall outward transport of moisture (Tab. 1). The values into ASC_i are higher. The difference of these numbers in C21 and C20 is statistically significantly different from zero at the 99.5 % level according to a t-test based on the instantaneous transports of all time steps. Although the increase of inward and outward directed transports counteract the projected increase in the budget also is statistically significantly different from zero at the 99.5 % level.

Based on the vertical profile we have separated the transports below RL and above, and calculated time series of the vertically aggregated yearly mean transports into ASC (positive values) below and of the vertically aggregated yearly mean transport out of ASC (negative values) above the reversal level in each of the experiments (Fig. 4). Like the total transports, both the lower level inward as well as the mid-level outward transports are projected to strengthen considerably in a warmed future. The change again is statistically significantly different from zero at 99.5% and results in an intensified hydrological cycle. The percentage increase of the outward transport above RL (Fig. 4(b), $MT_{out} \approx 38\%$) is more than twice as large as the inward transport below RL (Fig. 4(a), $MT_{in} \approx 17\%$) in both experiments. This highlights the importance of the mid-level outward transports and that water from ASC may be recycled in DESC. Thus it may modify simplistic views on precipitation change in which precipitation in the moist tropics is assumed to scale with low-level tropospheric water vapor and thus basically with low level moisture inflow only, as e.g. in Held and Soden (2006). The higher percentage increase in the outward moisture transport can be explained from theoretical considerations: following the Clausius-Clapeyron equation (Wentz and Schabel 2000; Held and Soden 2006) moisture content at the higher (and thus colder) levels experience a higher percentage change than at the warmer lower levels (Allan 2012), which is in line with our data (Fig. 5).

Despite the increasing outward transports, a statistically significant increase is found for the budget ($MT_{in} - MT_{out}$), which, assuming a negligible increase in total atmospheric water storage, determines the change of precipitation minus evaporation over the tropics. Thus, in line with previous studies (Wentz et al. 2007; Stephens and Ellis 2008; Allan et al. 2010; Liu and Allan 2012), tropical precipitation increases following our data. The contribution of moisture transports to this increase is about 15% from our C20 towards C21 based on the absolute increase of the budget for both, ASC_i as well as ASC_m.

Additionally to a strengthening of the hydrological cycle from C20 towards C21, we also found an acceleration of the strengthening. Significant changes were not found for the C20 period, in accordance with simulations by ERA-interim (Dee et al. 2011; Zahn and Allan 2011), but there is a statistically significant trend over the 31 year C21 period (at 99.5% level for the ASC_i budget, 97.5% for the ASC_m budget).

Previous studies (Wentz et al. 2007; Stephens and Ellis 2008; Allan et al. 2010) have not only suggested an increase in the mean tropical precipitation as a response to a warmed atmosphere, but especially a response in the higher percentiles of the distribution of precipitation events (Kharin et al. 2007; Allan and Soden 2008), commonly referred to as extreme events. To supply water for these events moisture transport must also have increased in the upper percentiles. The x-percentile is a threshold value above which x% of the observations (in our case simulated instantaneous moisture transports) are situated. We here used for each experiment the mean moisture transport over the boundary into ASC_i at each output time. Thus percentiles are calculated based on populations of more than 45000 observations, i.e. model time steps of C20 and C21 (Fig. 6(a) and Fig. 6(b)). Their change over the projected century of warming is shown in Fig. 6(c).

We find the most pronounced change in the highest percentiles of the low level inward transport and of the mid-level outward transport (compare large gaps between green and red line, which denotes the same 2% interval as green and blue line, respectively). The amount of increase of the strongest inward transport events (increase of 99%tile is $0.01629 kg * s^{-1} *$

m^{-1}) is not counteracted by the same amount of outward transport (increase of 99%tile is $-0.00183 kg * s^{-1} * m^{-1}$), which is in the order of ten times smaller. While there is a near linear increase between the 20%-80% percentiles, the upper end percentiles of moisture transport events increase at a greater rate (Fig. 7), resulting in greater precipitation rates during these extreme events.

Influence of changing wind and humidity

The moisture transports depend on two measures, the wind vectors and the atmospheric water content along the border separating ASC and DESC. Consequently, changes in the transport are provoked by changes in either of these two measures. In line with the Clausius-Clapeyron equation (Wentz and Schabel 2000; Held and Soden 2006), precipitable water has increased with warming throughout the atmosphere over all percentiles (Fig. 8(a)) from C20 to C21. While the relative increase is stronger in the upper atmosphere (Fig. 5), the absolute amount of change is strongest at low levels, and decreases with height.

The situation is different for the wind. We here use a measure for the wind circulation strength independent from the actual level thickness and named 'effective wind' previously (Sohn and Park 2010), which is the wind at a given level (between its upper and lower surface) weighted by the fraction of moisture held within this level. We found, that for the lower level inward transport below approximately 800 hPa, the effective wind is projected to weaken. Above 800 hPa until about 600 hPa, at the vertical levels at which most of the outward transport takes place, the change is positive, meaning a weakened wind contribution to the outward transport is projected. Only above, there are some levels projected to see an enhanced effective wind. We conclude the projected increase of the strength of the hydrological cycle is caused by higher humidity rather than circulation strength.

Influence of northern and southern boundary of ASC

The major part of the moisture is transported into ASC meridionally, following the lower branch of the Hadley Circulation. Although some events occasionally are directed the opposite way we find this Hadley pattern is represented generally very well at our southern boundaries (Fig. 9). The situation at the northern boundary is more complex and the median (50% percentile) is only slightly above 0.

Generally the southern boundary inward transports dominate those at the northern boundary by far, which may be due to the distribution of land-sea mass across the globe. Northern boundaries of ASC are much more likely to be situated over land than the southern ones. Over land, however, air carries lower amounts of water due to lower supply by evaporation and circulation patterns are much more influenced by orography and thus much more complex, e.g. directed northward opposite the main flow even at low levels. Over the course of a warming 21st century a widening of the percentiles of lower level inward and outward transport (recall the instantaneous transports do not always follow the idealized vertical shape of the Hadley Circulation) events are observed at both, the northern as well as the southern boundary. However the median only increases (by almost a quarter) at the southern boundary, whereas the already low value at the northern boundary gets even smaller. Thus the domination of the southern boundary for the moisture transports into ASC increases.

Changes of ASC/DESC pattern

There may be an influence of the latitude ASC is located at since regions closer to the equator are normally warmer and thus air does carry more moisture here, allowing for larger moisture transports. We found large changes of the frequency a particular grid box belongs to ASC in the two experiments, ASC_i and ASC_m, with minor changes in few areas only (white in Fig. 10(a)). The changes are about three times more distinct for ASC_m. Along the equatorial oceans spans an area of increasing likelihood to belonging to ASC, indicating more frequent convection. North and south are some areas, especially in ASC_m (Fig. 10(b)), with less frequent upward vertical wind velocity. This suggests a narrowing of the ITCZ in these regions, shifting their borders equatorward to warmer latitudes enhancing the transports in addition to the already warming atmosphere. This narrowing becomes more obvious when the zonal mean frequencies of a grid box belonging to ASC are looked at (Figs. 10(c) and 10(d)). For ASC_i, the ASC/DESC pattern is not very distinct, and there are few changes visible from C20 towards C21. For ASC_m a distinct ASC/DESC pattern is visible. If one assumes a certain threshold to separate dry and moist regions in the tropics, e.g. moist gridboxes must belong the ASC 40% of the time, there is a narrowing of the ITCZ. A narrowing of the ITCZ does not necessarily oppose the findings of a widening of the Hadley Cell by (Lu et al. 2007; Previdi and Liepert 2007), since they use a different measure and estimate the latitude of maximum down draft (stream function is zero) in the dry sub tropics. However, it highlights the sensitivity of any measure to the methods appplied. A narrowing may even be in line with the 'upped-ante mechanism' proposed before, in which relatively dry low-level advection into the ITCZ (Lintner and Neelin 2007) may lead to an inward shift of the margins of the convective regions (Chou et al. 2009).

There are major areas of less frequent ascending air movement over the Indonesian islands, the up-draft region of the Walker Circulation. Associated with the Walker Circulation is a down-draft of air masses over the tropical Pacific. Our findings suggest a weakening of the Walker Circulation, with less frequent convection in its up-drafting and more frequent convection in its down-drafting branch in a warmed atmosphere, in line with previous studies (Vecchi et al. 2006; Merlis and Schneider 2011) and with a weakening of zonal tropical circulations with warming in general (Vecchi and Soden 2007).

4. Discussion

In this study we investigated changing tropical moisture transports associated with future climate warming. We used data from a high space and time $(0.5°, 6h)$ resolution IPCC-AR4 model. As done in most studies applying mean data we estimated moisture transports into mean regions of air ascend, representative for regions referred to as the moist tropics or the ITCZ. However our high resolution data also enabled us to calculate instantaneous moisture transports into individual convective regions. In doing so we link instantaneous vertical wind with instantaneous humidity and horizontal wind, which is physically more consistent than linking mean and instantaneous variables.

This may be illustrated by the transports for the example field in Fig. 1(a). When the instantaneous wind and humidity field of 22 Mar 1965, 6:00am is applied to ASC_m of March, most of the boundary segments of ASC_m would not overlap with those of the instantaneous field. This means that most of the ASC_m boundary segments are not at the margins of the actual ASC_i, which are physically consistent with the distribution of instantaneous wind and humidity, but instead separate two DESC or two ASC grid boxes of the instantaneous field. As a consequence instantaneous moisture transports applied to ASC_m do not represent transports from DESC to ASC, but would be calculated from wet to wet or from dry to dry grid boxes, and maybe even from wet to dry, but not from dry to wet along many of the boundary segments. We believe that such physically inconsistent mixing of mean and instantaneous values to calculate transports leads to the systematically different values in between the two experiments.

Using the high horizontal and vertical resolution data allowed us to investigate moisture transports at very high detail. The moisture budget of a region is determined by the in- and outward transports, which together constitute the circulation pattern. To fully understand changes of the moisture budget, changes of the in- and outward transports of moisture need to be understood. Here we can separate between lower level inward and mid-level outward transports and find both to have intensified, especially during extreme precipitation events. It has in recent studies been found that changes of the amount of precipitation from models do not scale well with observed ones (Allan and Soden 2007; Allan et al. 2010). Modeled increases in precipitation were found to be too weak in ASC, but the observed decline in DESC was too weak as well. One may speculate, that models overestimate the mid-level outward transports which leads or at least contributes to such behavior. This may be caused by too high humidity values at the mid-levels due to too weak moist convection parametrisation schemes in the tropics, which may not 'rain out' enough of the atmospheric water. Different convection schemes have been suggested to cause large inter model spread for precipitation scaling (O'Gorman and Schneider 2009). However it can not be verified that mid-level humidity values are too high at this point since comprehensive 3-d humidity data for the atmosphere are not available.

Unlike previous studies for the recent past, which found the influence of humidity change to be of minor and the wind contribution to be of higher importance (Sohn and Park 2010; Zahn and Allan 2011), we here for a projected future change found the opposite. Moisture transport changes are mainly found to be due to higher atmospheric humidity values, and not to changing wind characteristics which were rather found to have weakened. However, the two reanalysis based studies span relatively short time periods only with small temperature increases and the signal of change may be influenced by short term variability.

A somewhat surprising finding is a narrowing of the ITCZ in our data, since previous studies have suggested a widening of the Hadley Cell (Lu et al. 2007; Previdi and Liepert 2007). A straightforward assumption would have been a widening of the ITCZ as well. However our results use a different measure and are only based on one model and are not statistically significant, yet, but we think it would be interesting to investigate this in more detail.

Even more surprising is the fact that applying the same data we get different answers whether the ITCZ has expanded depending on if we apply instantaneous or temporally averaged vertical wind. The different changes may be explained by a non Gaussian distribution of vertical wind speeds (Emori and Brown 2005). Grid cells, which are frequented by strong convective cells (with high upward ω) only at a few time steps are rarely assigned to ASC_i, but will be assigned to ASC_m when the upward ω at these few situations is high enough to out-range the otherwise low intensity down-draft situations in the averaging. One may speculate that some extremely intensive convective cells from more intense tropical storms in a warmed atmosphere (Bengtsson et al. 2007; Knutson et al. 2010) may cause the differently pronounced change between ASC_i and ASC_m.

5. Summary

We demonstrate, using high time and space resolution simulations, a strengthening of the water exchange into and out of the ascending regions of the tropics with climate warming, consistent with an intensified hydrological cycle. This is valid for the lower level inward transports as well as for the mid-level outward one. The response is particularly pronounced for the highest percentiles of moisture transport, indicating an intensification in the extremes of precipitation. The changes are mainly caused by higher atmospheric humidity values, and the wind contribution has minor, dampening effect. Finally we show that averaging data may lead to different results on changes in the ITCZ.

Acknowledgments.

The simulations were performed with the ECHAM5 model developed at the Max-Planck Institute for Meteorology, Germany, at HLRN (Norddeutscher Verbund für Hoch und Höchstleistungsrechne

We are thankful to Noel Keenlyside and Kevin Hodges for help with these data and for discussions. M.Z. was funded by the NERC PREPARE project, NE/G015708/1.

REFERENCES

Allan, R., 2012: The role of water vapour in earths energy flows. *Surveys in Geophysics*, 1–8, URL `http://dx.doi.org/10.1007/s10712-011-9157-8`, 10.1007/s10712-011-9157-8.

Allan, R. P. and B. J. Soden, 2007: Large discrepancy between observed and simulated precipitation trends in the ascending and descending branches of the tropical circulation. *Geophys. Res. Lett.*, **34 (L18705)**, doi:10.1029/2007GL031460.

Allan, R. P. and B. J. Soden, 2008: Atmospheric warming and the amplification of precipitation extremes. *Science*, **321**, 1481–1484.

Allan, R. P., B. J. Soden, V. O. John, W. Ingram, and P. Good, 2010: Current changes in tropical precipitation. *Environmental Research Letters*, **5 (2)**, 025 205, URL `http://stacks.iop.org/1748-9326/5/i=2/a=025205`.

Allen, M. R. and W. J. Ingram, 2002: Constraints on future changes in climate and the hydrologic cycle. *Nature*, **419**, 224–232.

Bengtsson, L., 2010: The global atmospheric water cycle. *Environ. Res. Lett.*, **5 (025202)**, doi:doi:10.1088/1748-9326/5/2/025202.

Bengtsson, L., K. I. Hodges, M. Esch, N. Keenlyside, L. Kornblueh, J.-j. Luo, and T. Yamagata, 2007: How may tropical cyclones change in a warmer climate? *Tellus*, **59**, 539–561, doi:10.1111/j.1600-0870.2007.00251.x.

Bigg, G. R., 2006: Comparison of coastal wind and pressure trends over the tropical atlantic: 1946-1987. *Int. J. Climatol.*, **13**, 411–421, doi:DOI:10.1002/joc.3370130405.

Chou, C. and C.-A. Chen, 2010: Depth of convection and the weakening of tropical circulation in global warming. *J. Climate*, **23**, 30193030, doi:doi:http://dx.doi.org/10.1175/2010JCLI3383.1.

Chou, C., J. D. Neelin, C.-A. Chen, and J.-Y. Tu, 2009: Evaluating the rich-get-richer mechanism in tropical precipitation change under global warming. , 1982-2005. *J. Climate*, **22**, doi:http://dx.doi.org/10.1175/2008JCLI2471.1.

Chou, C., J. Tu, and P. Tan, 2007: Asymmetry of tropical precipitation change under global warming. *Geophys. Res. Lett.*, **34 (L17708)**, doi:10.1029/2007GL030327.

Dee, D. P., et al., 2011: The ERA-interim reanalysis: configuration and performance of the data assimilation system. *Quarterly Journal of the Royal Meteorological Society*, **137 (656)**, 553–597, doi:10.1002/qj.828, URL `http://dx.doi.org/10.1002/qj.828`.

Emori, S. and S. J. Brown, 2005: Dynamic and thermodynamic changes in mean and extreme precipitation under changed climate. *Geophys. Res. Lett.*, **32 (L17706)**, doi:10.1029/2005GL023272.

Gastineau, G. and B. J. Soden, 2009: Model projected changes of extreme wind events in response to global warming. ,, doi:. *Geophys. Res. Lett.*, **36 (L10810)**, doi:10.1029/2009GL037500.

Held, I. M. and B. J. Soden, 2006: Robust responses of the hydrological cycle to global warming. *J. Climate.*, **19**, 5686–5699.

John, V. O., R. P. Allan, and B. J. Soden, 2009: How robust are observed and simulated precipitation responses to tropical ocean warming? *Geophys. Res. Lett.*, **36 (L14702)**.

Kharin, V. V., F. W. Zwiers, X. Zhang, and G. C. Hegerl, 2007: Changes in temperature and precipitation extremes in the IPCC ensemble of global coupled model simulations. *J. Climate*, **20**, 14191444, doi:doi:http://dx.doi.org/10.1175/JCLI4066.1.

Knutson, T. R., et al., 2010: Tropical cyclones and climate change. *Nature Geoscience*, **3**, 157 – 163, doi:10.1038/ngeo779.

Lenderink, G. and E. van Meijgaard, 2008: Increase in hourly precipitation extremes beyond expectations from temperature changes. *Nature Geoscience*, **1**, doi:10.1038/ngeo262.

Lintner, B. R. and J. D. Neelin, 2007: A prototype for convective margin shifts. *Geophys. Res. Lett.*, **34 (L05812)**, doi:doi:10.1029/2006GL027305.

Liu, C. and R. P. Allan, 2012: Multi-satellite observed responses of precipitation and its extremes to interannual climate variability. *J. Geophys. Res.*, **117 (D03101)**, doi:doi:10.1029/2011JD016568.

Lu, J., G. A. Vecchi, and T. Reichler, 2007: Expansion of the Hadley cell under global warming. *Geophys. Res. Lett.*, **34 (L06805)**, doi:doi:10.1029/2006GL028443.

Merlis, T. M. and T. Schneider, 2011: Changes in zonal surface temperature gradients and walker circulations in a wide range of climates. *J. Climate*, **24**, 47574768., doi:http://dx.doi.org/10.1175/2011JCLI4042.1.

Nakicenovic, N. and R. Swart, (Eds.) , 2000: *IPCC Special Report on Emissions Scenarios*. Cambridge Univ. Press.

O'Gorman, P. A. and C. J. Muller, 2010: How closely do changes in surface and column water vapor follow ClausiusClapeyron scaling in climate change simulations? . *Environmental Research Letters*, **5 (025207)**, doi:doi:10.1088/1748-9326/5/2/025207.

O'Gorman, P. A. and T. Schneider, 2009: The physical basis for increases in precipitation extremes in simulations of 21st-century climate change. *Proc. Nat. Acad. Sci.*, **106**, 14 773–14 777.

Power, S. B. and I. N. Smith, 2007: Weakening of the Walker Circulation and apparent dominance of El Niño both reach record levels, but has ENSO really changed? *Geophys. Res. Lett.*, **34 (L18702)**, doi:doi:10.1029/2007GL030854.

Previdi, M. and B. G. Liepert, 2007: Annular modes and hadley cell expansion under global warming. *Geophys. Res. Lett.*, **34 (L22701)**, doi:10.1029/2007GL031243.

Roeckner, et al., 2003: The atmospheric general circulation model ECHAM 5. PART I: Model description. *MPI-Report No 349*.

Seager, R., N. Naik, and G. A. Vecchi, 2010: Thermodynamic and dynamic mechanisms for large-scale changes in the hydrological cycle in response to global warming. *Journal of Climate*, **23 (17)**, 4651–4668, doi:10.1175/2010JCLI3655.1, URL `http://journals.ametsoc.org/doi/abs/10.1175/2010JCLI3655.1`, `http://journals.ametsoc.org/doi/pdf/10.1175/2010JCLI3655.1`.

Sohn, B. J. and S.-C. Park, 2010: Strengthened tropical circulations in past three decades inferred from water vapor transport. *J. Geophys. Res.*, **11**.

Stephens, G. L. and T. D. Ellis, 2008: Controls of global-mean precipitation increases in global warming GCM experiments. *J. Climate*, **21**, 61416155, doi:doi:http://dx.doi.org/10.1175/2008JCLI2144.1.

Trenberth, K. E., A. Dai, R. M. Rasmussen, and D. B. Parsons, 2003: The changing character of precipitation. *Bull. Amer. Met. Soc.*, **84**, 1205–1217.

Trenberth, K. E., L. Smith, T. Qian, A. Dai, and J. Fasullo, 2007: Estimates of the global water budget and its annual cycle using observational and model data. *J. Hydrometeor*, **8**, 758769, doi:doi:http://dx.doi.org/10.1175/JHM600.1.

Vecchi, G. A. and B. J. Soden, 2007: Global warming and the weakening of the tropical circulation. *J. Climate*, **20**, 4316–4340, doi:doi:http://dx.doi.org/10.1175/JCLI4258.1.

Vecchi, G. A., B. J. Soden, A. T. Wittenberg, I. M. Held, A. Leetmaa, and M. J. Harrison, 2006: Weakening of tropical pacific atmospheric circulation due to anthropogenic forcing. *Nature*, **441**, 73–76, URL http://dx.doi.org/10.1038/nature04744.

Wentz, F. J., L. Ricciardulli, K. Hilburn, and C. Mears, 2007: How much more rain will global warming bring? *Science*, **317**, 233 – 235.

Wentz, F. J. and M. Schabel, 2000: Precise climate monitoring using complementary satellite data sets. *Nature*, **403**, 414–416, doi:doi:10.1038/35000184.

Zahn, M. and R. P. Allan, 2011: Changes in water vapor transports of the ascending branch of the tropical circulation. *J. Geophys. Res.*, **116 (D18111)**, doi:doi:10.1029/2011JD016206.

List of Tables

TABLE 1. Average of inward (MTin) and outward (MTout) moisture transport in C20 and C21. Values are based on instantaneous transports at all the n_b boundary segments and all n_l vertical vertical levels at all time steps t (confer1). To calculate the inward/outward transport, transports at all boundary segments are used which are directed inward/outward of ASC (positive/negative courves in Fig. 3).Unit is $[kg * s^{-1} * m^{-1}]$.

	$MTin$	MTout	budget
$C20_m$	83.25	-77.95	5.30
$C21_m$	102.72	-96.91	5.82
$C20_i$	87.710	-79.57	8.14
$C21_i$	110.54	-101.42	9.12

List of Figures

10 **Changing frequency of the ascending regions.** (a) Change of percentage of time steps a grid box belongs to ASC from the instantaneous vertical wind (ASC_i), C21 - C20. (b) Change of percentage a grid box belongs to ASC when derived from the monthly mean vertical wind (ASC_m), C21 - C20. Red indicates a box belongs to ASC more frequently, blue means it belongs to ASC less frequently. Note the different scale of the colour bar. (c)/ (d) Zonal mean percentage a grid box belongs to ASC_i/ASC_m. Green denotes C21, red C20. 35

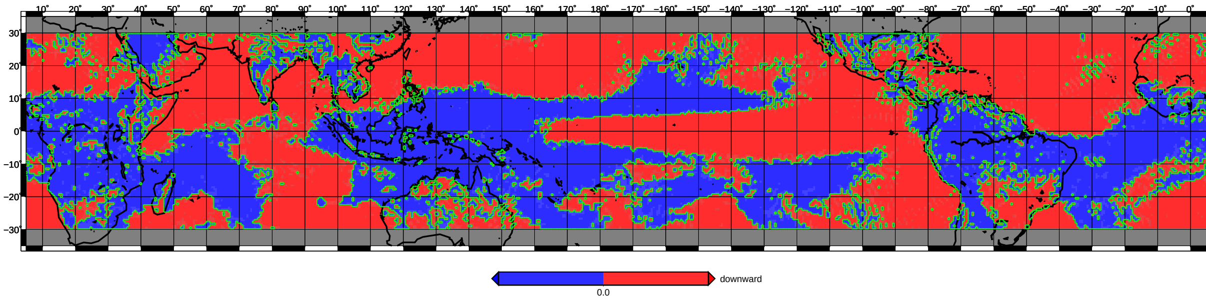

(a) ASC_m Mar 1965

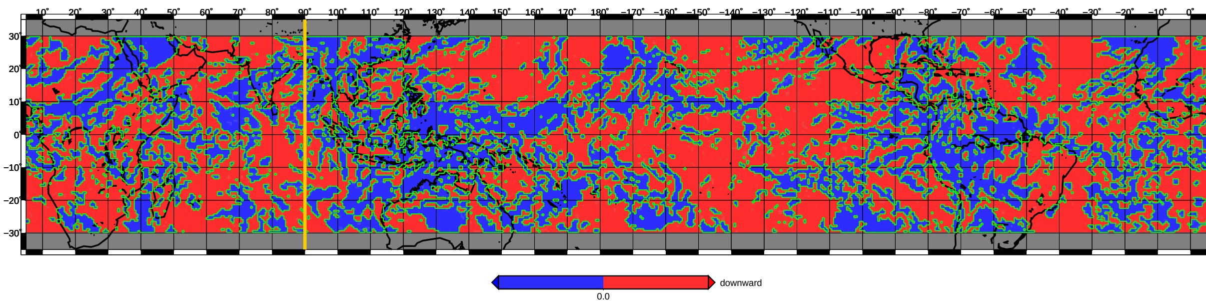

(b) ASC_i 22 Mar 1965, 6:00am

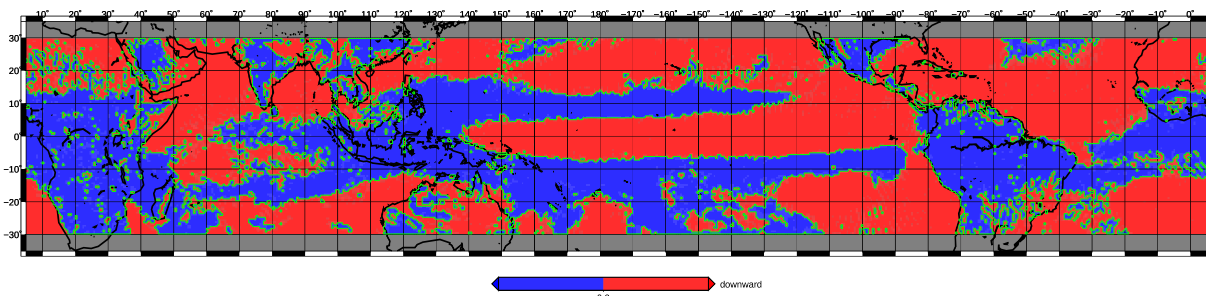

(c) ASC_m Mar 2075

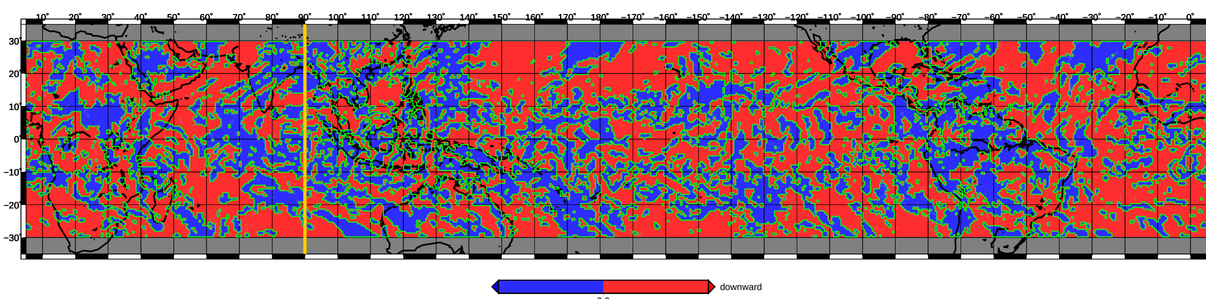

(d) ASC_i 22 Mar 2075, 6:00am

FIG. 1. **Example fields of $\mathbf{ASC_i}$ and of $\mathbf{ASC_m}$ in C20 and C21.** Distribution of ascending and descending regions from ECHAM5, red denotes down-draft, blue denotes up-draft, green is the boundary line across which fluxes are calculated. (a) valid March 1965, (b) valid 22 March 1965, 6:00am, (c) valid March 2075 and (d) valid 22 March 2075, 6:00am.

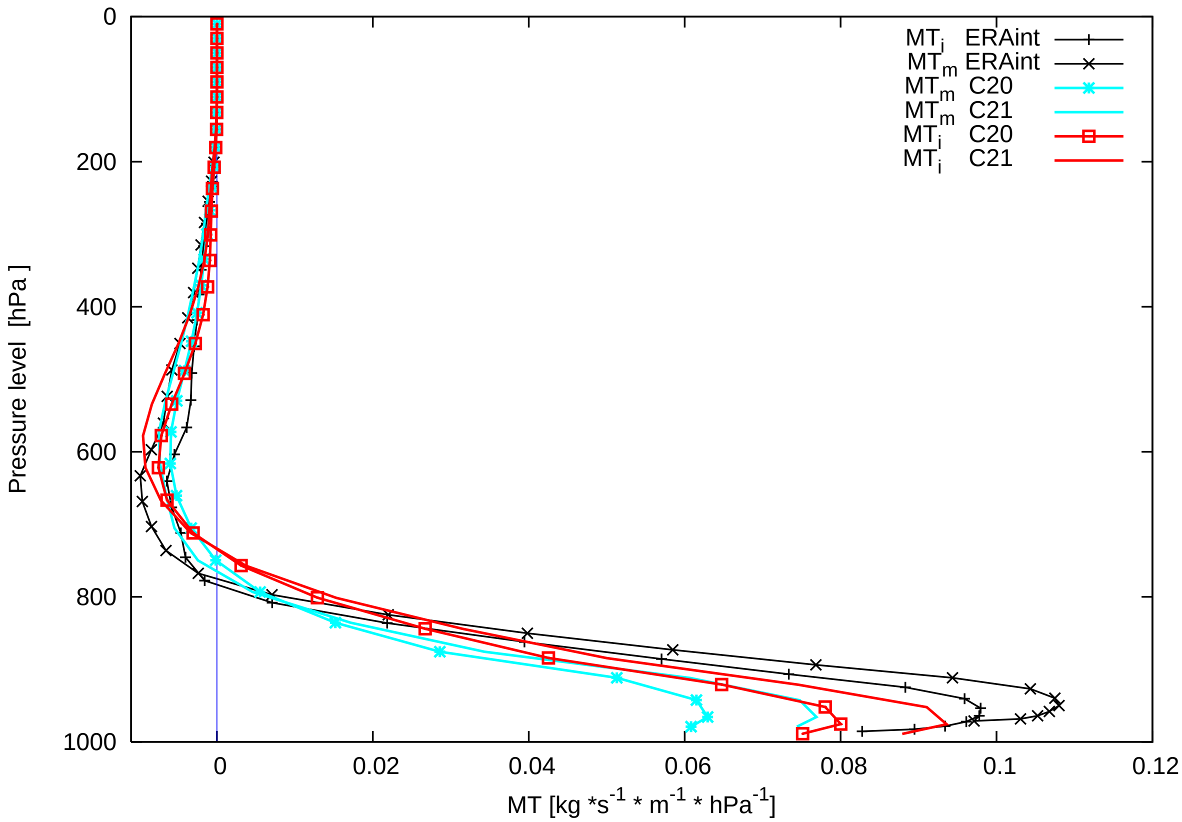

FIG. 2. **Vertical profiles of horizontal moisture transports.** Magnitude of horizontal net moisture transport per hPa along ASC/DESC boundary from ECHAM5 and ERA-interim (Dee et al. 2011; Zahn and Allan 2011) into ASC_i and ASC_m. Positive/negative values denote net transports into/out of ASC. Symbols denote locations of mean pressure and mean transports. Unit of transport is mass of water [kg] per time [s] and area $[hPa * m]$. Note that the vertical unit of the area is given in pressure [hPa].

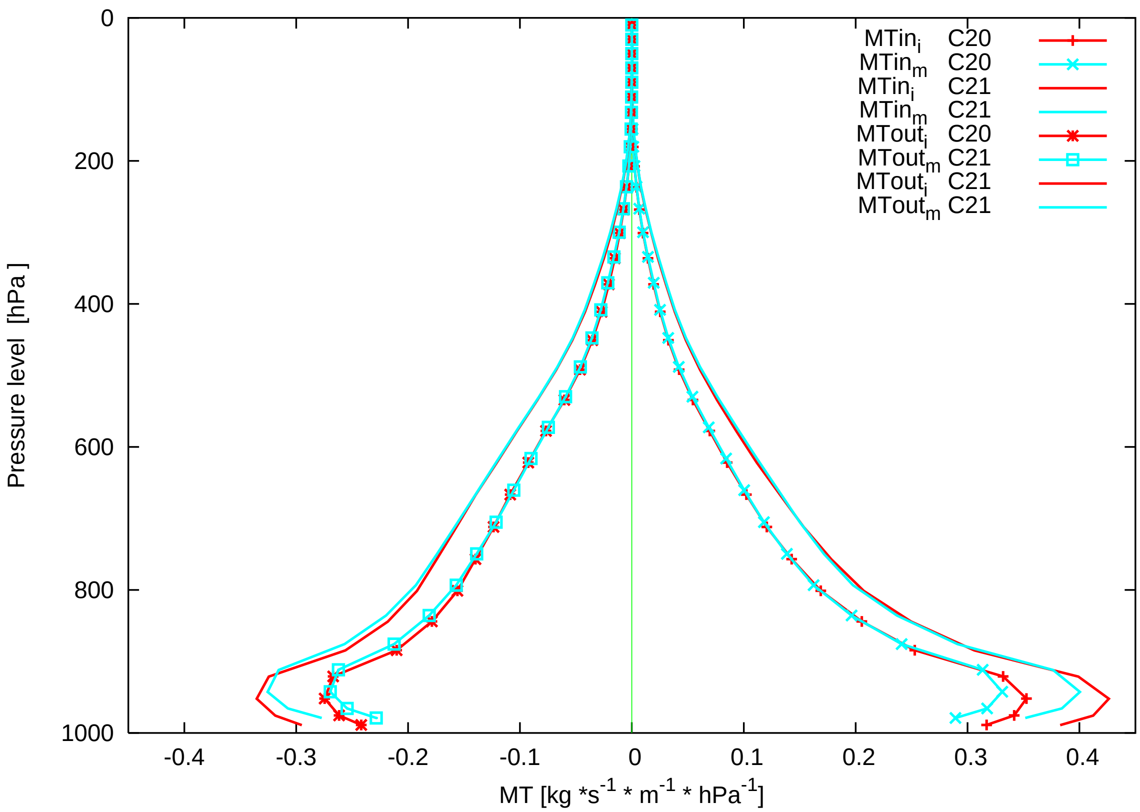

FIG. 3. **Vertical profile of isolated inward and outward transport of moisture.** Curves on the left/right hand-side show the average vertical profile of isolated outward/inward only transport of moisture per height (negative/positive values) for the total period of the different experiments. Curves for C20 are denoted by lines with points, those for C21 are denoted by plain lines.

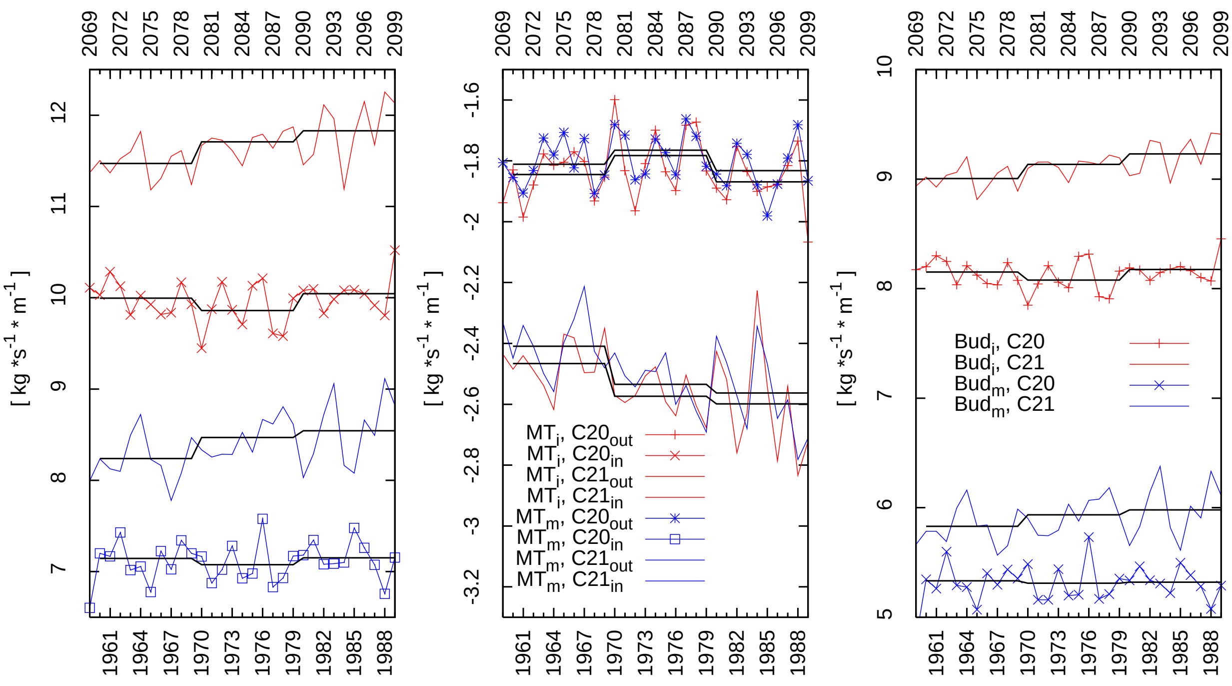

(a) MT_{in} (b) MT_{out} (c) Budget

FIG. 4. **Temporal evolution of moisture transport into the ascending region.** Times series of mean yearly moisture transports over ASC/DESC boundary below (a) and above (b) the reversal level. (c) time series of the yearly mean budget. C21 years refer to upper x-axis, C20 years refer to lower x-axis. Plain lines indicate C21 values, lines with symbols refer to C20 values. Flags for (a) are given in (b). Black lines indicate decadal means (1st, 2nd and 3rd decade of each data set), respectively.

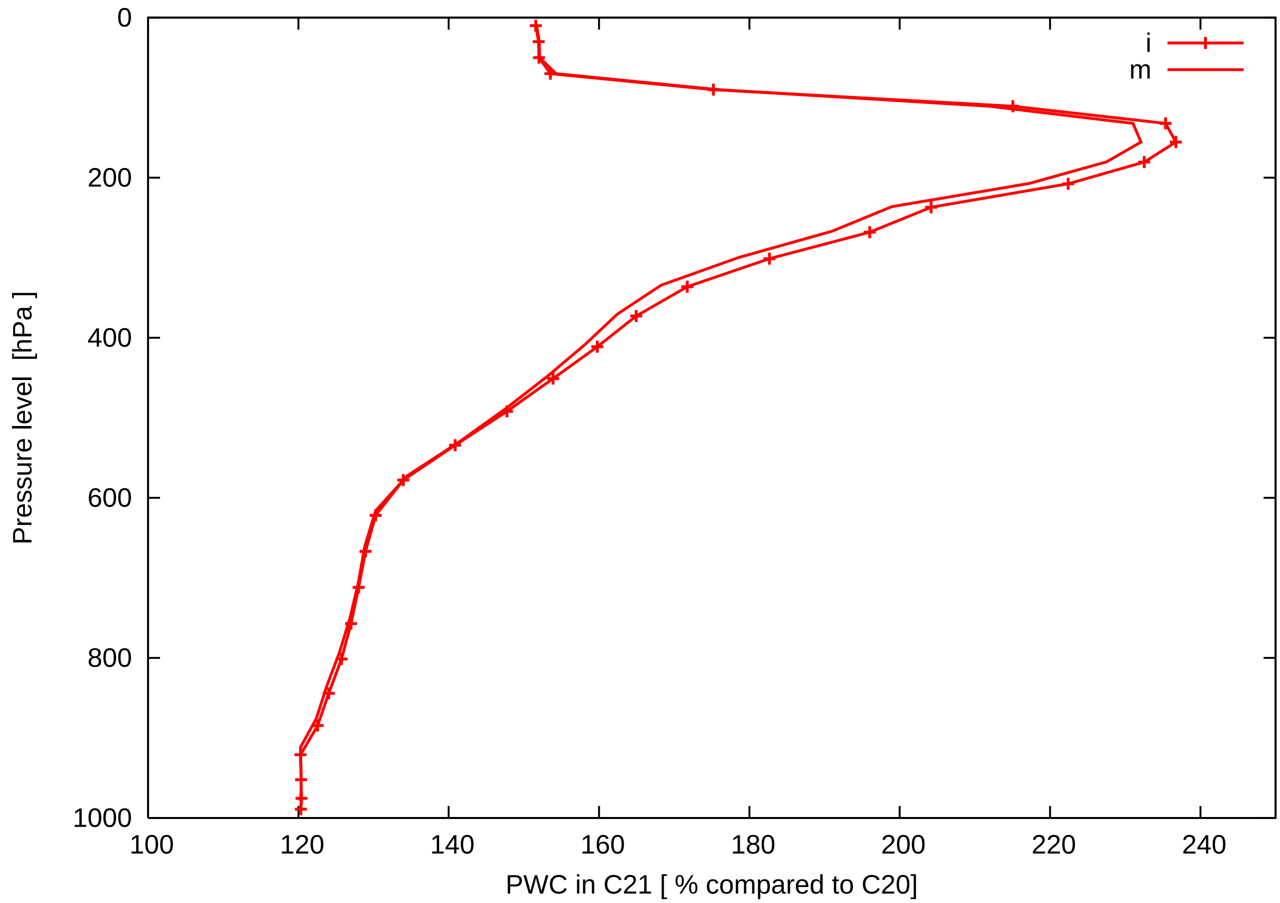

Fig. 5. **PWC along boundaries in C21 relative to C20.** Percentage of precipitable water content along ASC/DESC boundary of ASC_i and ASC_m in C21 relative to C20.

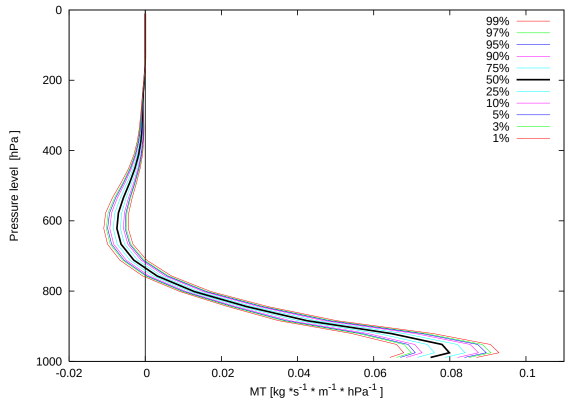

(a) C20

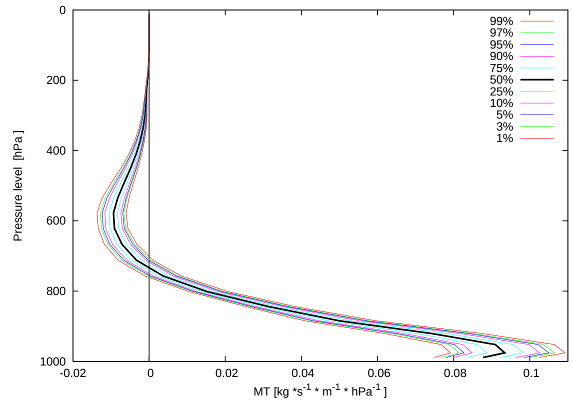

(b) C21

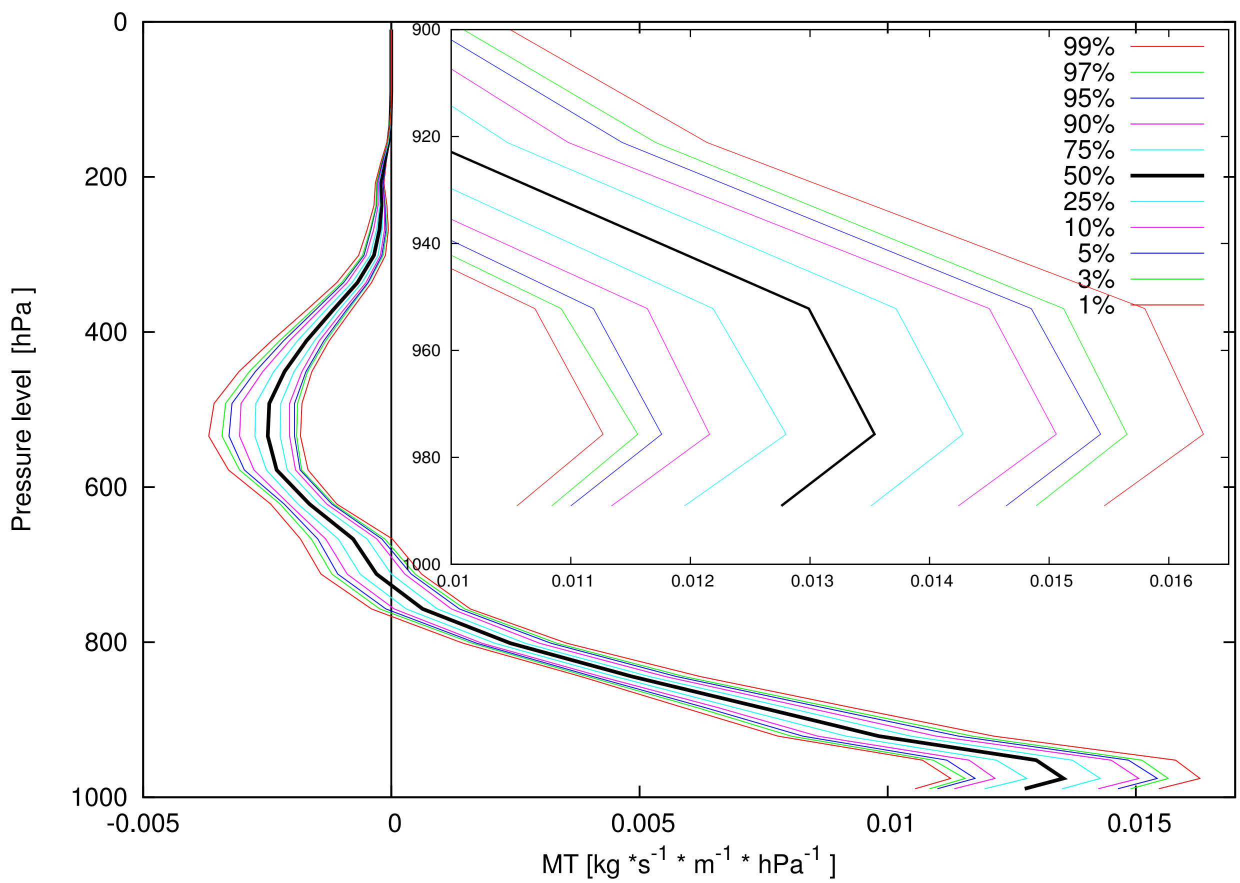

(c) C21 - C20

(c)

Fig. 6. **Vertical structure of percentiles of moisture transports.** Vertical structure of percentiles of moisture transports (a) for C20 and (b) for C21. (c) Vertical profile of the difference between both, C21 - C20. Lower right corner is enlarged.

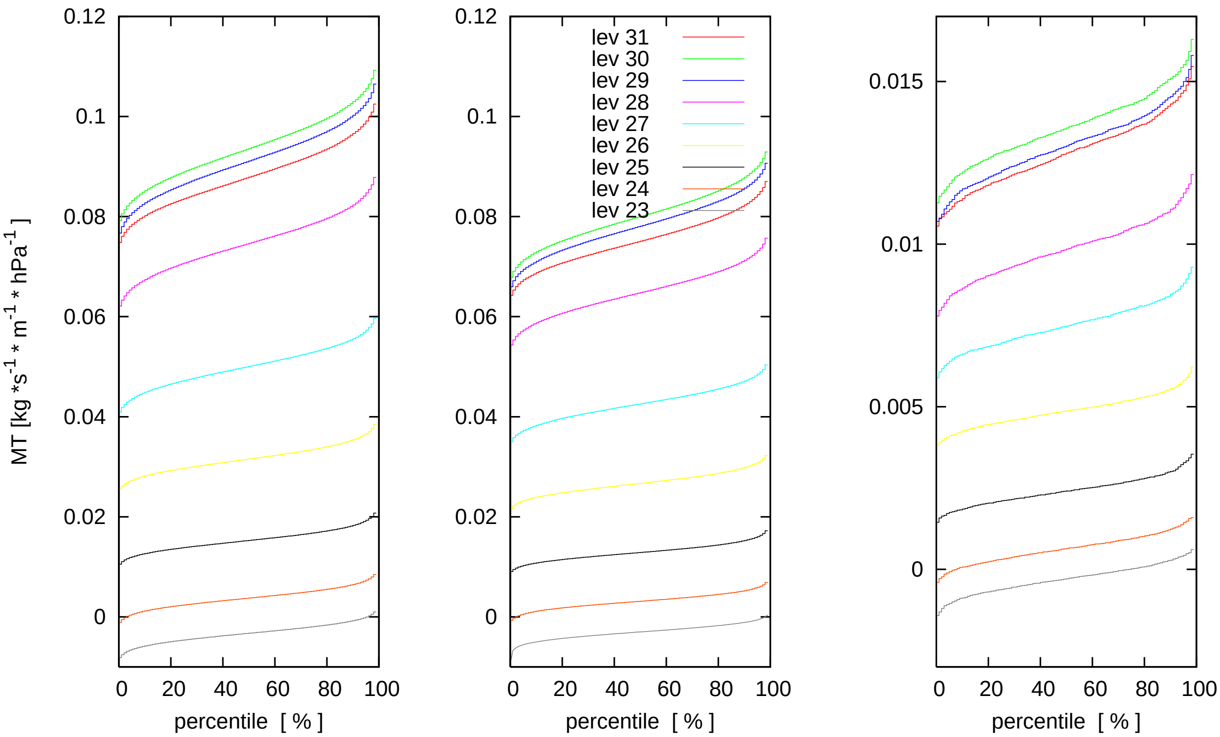

(a) C21 (b) C20 (c) C21 - C20

FIG. 7. **Percentiles of moisture transports at lower levels.** (a)Percentiles of moisture transports at lower levels for C21, (b) percentiles of moisture transports at lower levels for C20 and (c) difference of percentiles of moisture transports at lower levels, C21 - C20. Colours of levels in (b) are also valid for (a) and (c).

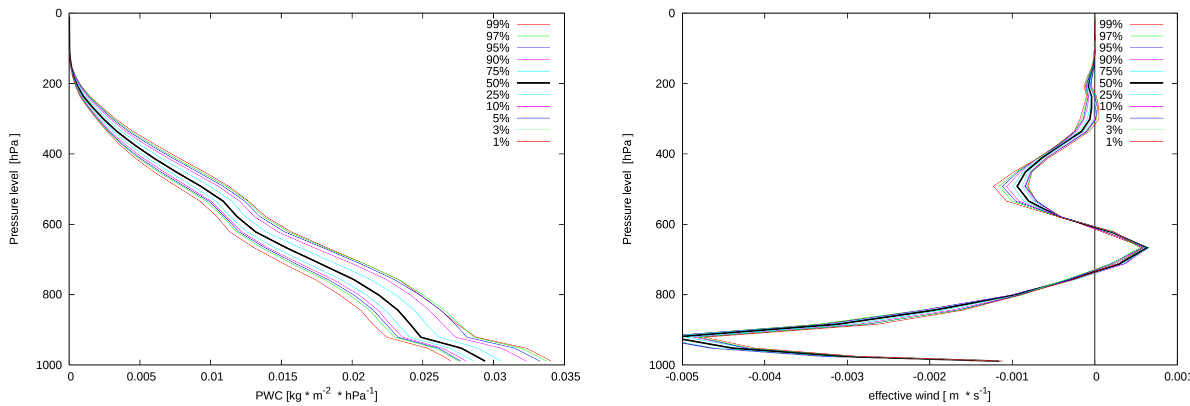

(a) PWC

(b) effective wind

Fig. 8. **Changes of percentiles of precipitable water and of effective wind along boundary of convective regions.** (a) Vertical profile of difference in the percentiles of precipitable water and (b) vertical profile of difference in the percentiles of the effective wind (C21 - C20, respectively). Here, effective wind is the mean wind directed towards ASC at a given level, weighted by the water content at the same level relative to the total column water content, following the definition of Sohn and Park (2010).

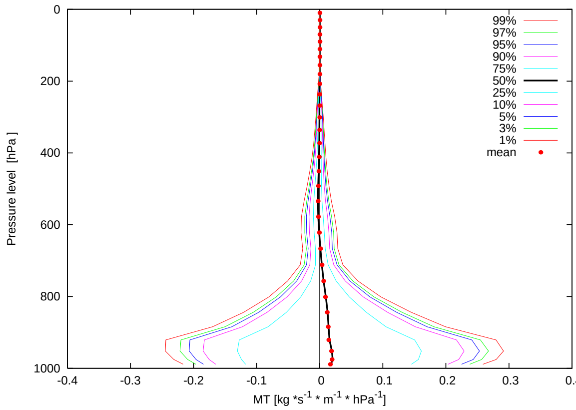

(a) at northern boundary, C20

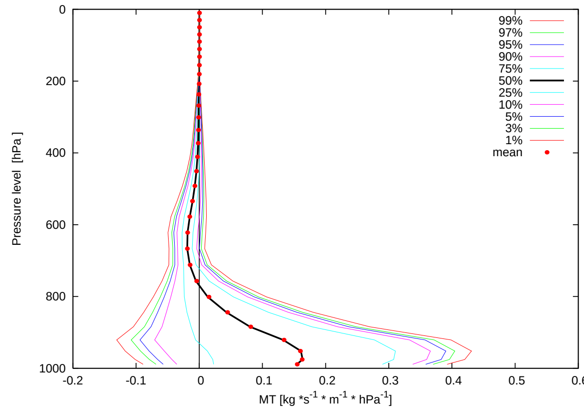

(b) at southern boundary, C20

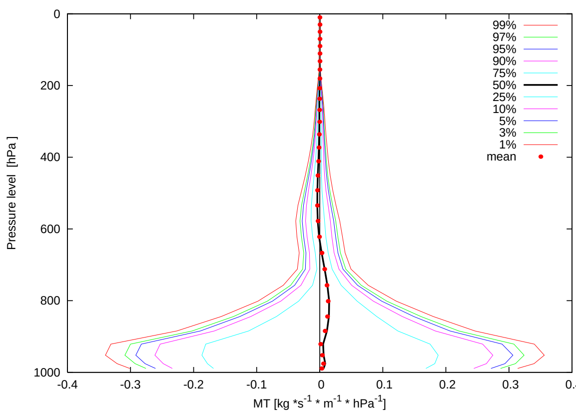

(c) at northern boundary, C21

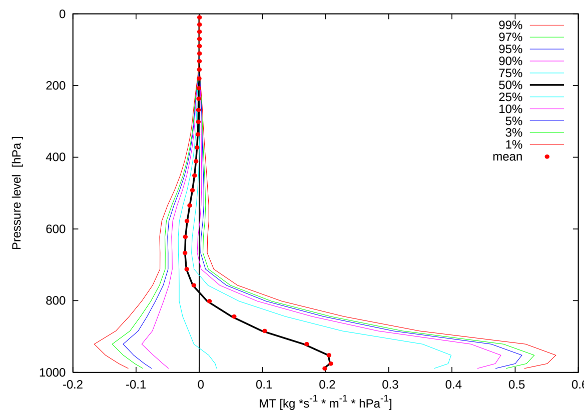

(d) at southern boundary, C21

FIG. 9. **Vertical structure of percentiles of moisture transports at northern and southern boundaries of $\mathbf{ASC_i}$.** (a) At the northern boundary in C20. (c) At the northern boundary in C21. (b) At the southern boundary in C20. (d) At the southern boundary in C21. Also given is the mean transport per hPa, respectively.

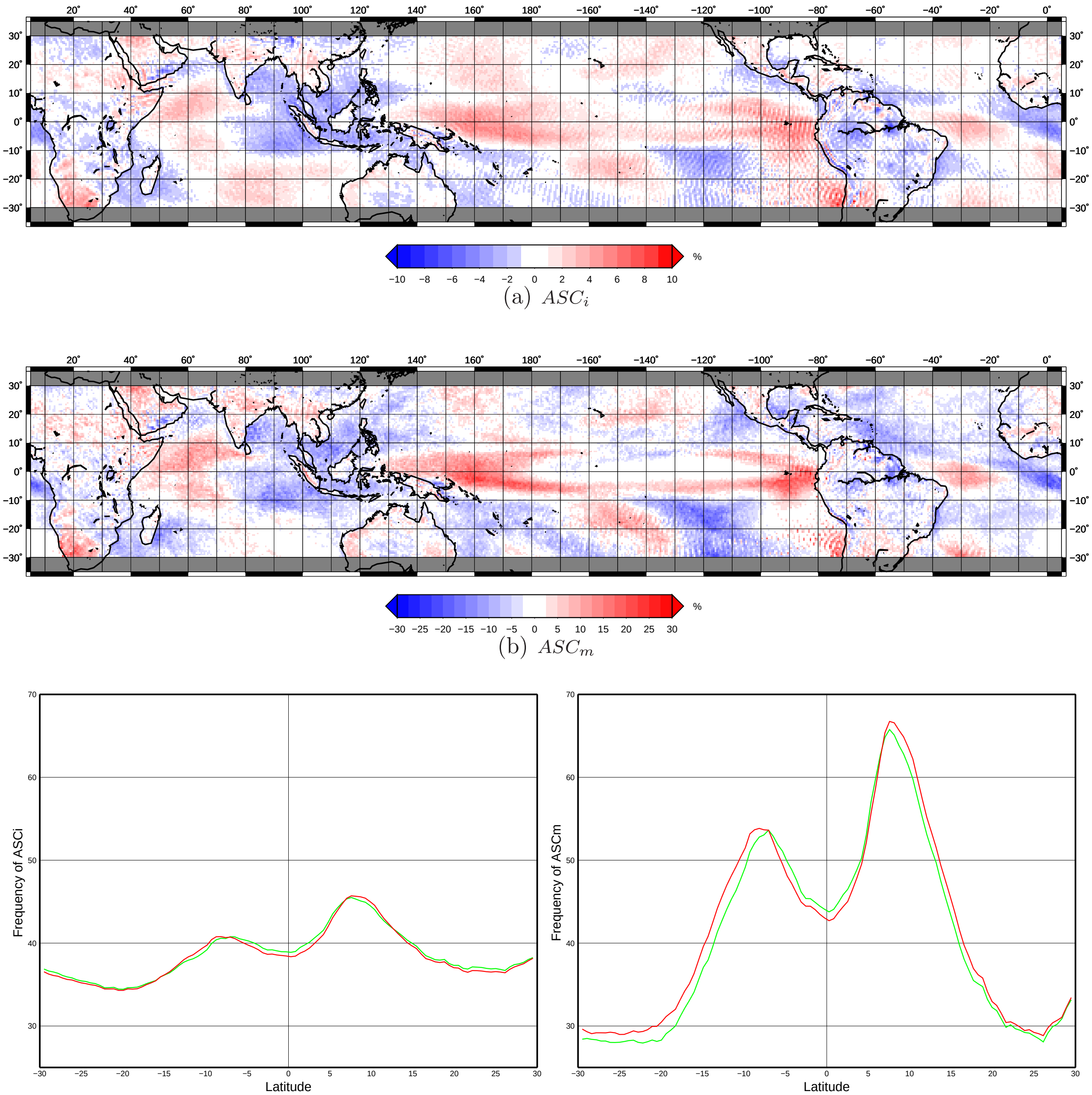

(a) ASC_i

(b) ASC_m

(c) zonal mean ASC_i

(d) zonal mean ASC_m

FIG. 10. **Changing frequency of the ascending regions.** (a) Change of percentage of time steps a grid box belongs to ASC from the instantaneous vertical wind (ASC_i), C21 - C20. (b) Change of percentage a grid box belongs to ASC when derived from the monthly mean vertical wind (ASC_m), C21 - C20. Red indicates a box belongs to ASC more frequently, blue means it belongs to ASC less frequently. Note the different scale of the colour bar. (c)/(d) Zonal mean percentage a grid box belongs to ASC_i/ASC_m. Green denotes C21, red C20.